**Journal Article**

# A Novel Compact Quadruple-Band Indoor Base Station Antenna for 2G/3G/4G/5G Systems

Q. Hua, Y. Huang, C. Song, M. O. Akinsolu, B. Liu, T. Jia, Q. Xu, and A. Alieldin

IEEE Access
Multidisciplinary | Rapid Review | Open Access Journal

Received September 4, 2019, accepted September 23, 2019, date of publication October 16, 2019, date of current version October 30, 2019.

*Digital Object Identifier 10.1109/ACCESS.2019.2947778*

# A Novel Compact Quadruple-Band Indoor Base Station Antenna for 2G/3G/4G/5G Systems

**QIANG HUA[1], YI HUANG[1], (Senior Member, IEEE), CHAOYUN SONG[1], (Member, IEEE), MOBAYODE O. AKINSOLU[2], (Member, IEEE), BO LIU[2], (Senior Member, IEEE), TIANYUAN JIA[1], QIAN XU[3], (Member, IEEE), AND AHMED ALIELDIN[1], (Member, IEEE)**

[1]Department of Electrical Engineering and Electronics, University of Liverpool, Liverpool L69 3GJ, U.K.
[2]Faculty of Arts, Science and Technology, Wrexham Glyndŵr University, Wrexham LL11 2AW, U.K.
[3]College of Electronic and Information Engineering, Nanjing University of Aeronautics and Astronautics, Nanjing 211106, China

Corresponding authors: Yi Huang (yi.huang@liverpool.ac.uk) and Bo Liu (b.liu@glyndwr.ac.uk)

This work was supported by the Rentian Group in China.

**ABSTRACT** This paper presents a quadruple-band indoor base station antenna for 2G/3G/4G/5G mobile communications, which covers multiple frequency bands of 0.8 – 0.96 GHz, 1.7 – 2.7 GHz, 3.3 – 3.8 GHz and 4.8 – 5.8 GHz and has a compact size with its overall dimensions of 204 × 175 × 39 $mm^3$. The lower frequency bands over 0.8 – 0.96 GHz and 1.7 – 2.7 GHz are achieved through the combination of an asymmetrical dipole antenna and parasitic patches. A stepped-impedance feeding structure is used to improve the impedance matching of the dipole antenna over these two frequency bands. Meanwhile, the feeding structure also introduces an extra resonant frequency band of 3.3 – 3.8 GHz. By adding an additional small T-shaped patch, the higher resonant frequency band at 5 GHz is obtained. The parallel surrogate model-assisted hybrid differential evolution for antenna optimization (PSADEA) is employed to optimize the overall quadruple-band performance. We have fabricated and tested the final optimized antenna whose average gain is about 5.4 dBi at 0.8 – 0.96 GHz, 8.1 dBi at 1.7 – 2.7 GHz, 8.5 dBi at 3.3 – 3.8 GHz and 8.1 dBi at 4.8 – 5.0 GHz respectively. The proposed antenna has high efficiency and is of low cost and low profile, which makes it an excellent candidate for 2G/3G/4G/5G base station antenna systems.

**INDEX TERMS** 2G/3G/4G/5G, base station antenna, compact antennas, optimization method, quadruple-band antennas.

## I. INTRODUCTION

The performance of mobile wireless communication systems would be degraded in indoor environments, undergrounds and tunnels. Special indoor base station antennas are required for these areas in order to improve the quality and performance of mobile communication systems [1]. In particular, multiband antennas with a relatively compact dimension that can cover 2G, 3G and 4G frequency bands (0.8 – 0.96 GHz and 1.7 – 2.7 GHz) are preferred for many indoor base stations. With the rapid growth of communication data capacity, the fifth-generation (5G) communication systems are being deployed from this year (2019) in many countries. Since 2016, the band from 3.4 – 3.8 GHz has been allocated for 5G trials in European Union (EU). China's Ministry of Industry and Information Technology (MIIT) announced that 3.3 – 3.4 (indoor only), 3.4 – 3.6 and 4.8 – 5.0 GHz bands were allocated for 5G services in 2017 [2]. Considering the extra 5G bands, it may bring significant challenges in designing the next-generation indoor base station antennas. For example, it will increase the complexity and physical dimension of the antenna after adding the 5G bands in together with the well-developed 2G/3G/4G band coverage. Therefore, a compact multiband antenna with wide frequency bands is preferred for base station applications to support 2G, 3G, 4G and 5G communication systems simultaneously without increasing the overall size and number of antennas. In other words, the new indoor base station antenna is required to cover the frequency bands of 0.8 – 0.96, 1.7 – 2.7, 3.3 – 3.8 and 4.8 – 5.0 GHz with a compact size and low profile.

In the last twenty years, a large number of base station antennas with different structures have been investigated and proposed. Compared with monopole antennas, dipole antennas are more attractive for base stations, because it is easier to provide dual-polarization (e.g., crossed dipole), which can increase system capacity and combating the issue of

The associate editor coordinating the review of this manuscript and approving it for publication was Lu Guo.

multipath fading [3]. A number of broadband dual-polarized dipole antennas have been developed for 2G/3G/4G systems operating in the band 1.71 – 2.69 GHz [4]–[10]. The broadband performance can be achieved by many methods, such as making slots on the radiating patch [4], [5], adding parasitic elements [5], [6], using shared-dipole structure [7], [8], or applying better feeding methods [9], [10]. In fact, multiband antennas could perform better than wideband antennas due to in-band interference for such applications. Therefore, many dual-broadband antennas have been proposed to cover both 0.8 – 0.96 GHz and 1.7 – 2.7 GHz [11]–[16]. To achieve the dual-band characteristics, the first way is to share an element for the lower band and upper band [11]; the second way is to use the different elements for the lower band and upper band which is often used for base station [12]–[16]. The second way is easier to adjust the down-tilt angles in the lower band and upper band, but the structure will become more complicated compared with the first way. At the moment, very few published papers have reported the triple-band base station antennas for 5G due to the design complexity [17].

To obtain the desired performance, antenna optimization is often an essential step. However, optimizers in existing commercial electromagnetic (EM) simulation tools have difficulties to achieve the desired performance for this antenna because of the complexity of the structure. Therefore, the parallel surrogate model-assisted differential evolution method for antenna synthesis (PSADEA) [18] is selected to optimize this antenna. PSADEA is the state-of-the-art in the SADEA algorithm family [18]–[21], while the first generation SADEA method [20] already showed clear advantages over popular antenna optimization methods and tools [22].

Compared to standard global optimization methods, the SADEA algorithm family is able to obtain better design quality and offers 3 to 20 times efficiency improvement [20]–[22]. The primary features in the SADEA algorithm family include differential evolution (DE) algorithm as the global search engine, Gaussian process as the machine learning technique for surrogate modeling and the surrogate model-aware evolutionary search framework [23] as the model management method. PSADEA is distinct from other SADEA versions through the complementary adoption of multiple DE mutation operators and reinforcement learning techniques to achieve an additional 1.5 to 3 times efficiency improvement and higher design solution quality even in the sequential mode [18], [19]. However, the whole base station antenna involves more than 40 design parameters and more than 10 specifications. Thus the time spent on Gaussian process surrogate modeling in PSADEA becomes long. To address this problem, design knowledge is used to separate the design parameters, and PSADEA is used to focus on 19 design parameters. A successful design is finally obtained.

Furthermore, in this paper, a compact quadruple-band indoor base station antenna is proposed. It covers 0.8 – 0.96 GHz, 1.7 – 2.7 GHz, 3.3 – 3.8 GHz and 4.8 – 5.0 GHz simultaneously, which means that it can support 2G/3G/4G/5G systems at the same time. Meanwhile, through the folded stepped impedance feeding structure, the antenna has a compact size, especially the height, which is only 204 × 175 × 39 mm$^3$. In addition, the radome of the antenna is also considered for practical applications.

The paper is organized as follows: Section II describes the geometry, components and fabrication of the proposed antenna. Section III illuminates the evolution of the proposed antenna. The measurement process and results are shown in Section IV. The conclusion is drawn in Section V.

## II. ANTENNA STRUCTURE

The outer structure of the proposed antenna is shown in Fig. 1, which is made of polyvinyl chloride (PVC) box (with relative permittivity $\varepsilon_r = 3$) and an aluminum reflector. The thicknesses of the PVC box and aluminum reflector are 2 mm and 1 mm respectively. Fig. 2 illustrates the inner structure of the proposed antenna, which looks complicated but is based on dipole antenna (to be discussed in next section). Twenty-one blue PVC cylinders are applied to support the aluminum structure and provide the essential gap distance between the different components. They also provide a robust structure of the antenna. In order to have a better understanding of the inner structure, it can be divided into four layers and four bent metal strips, as shown in Fig. 3. The first layer consists of three metal patches and two metal strips, which are parasitic and used to increase the bandwidth of the first and second band. The second layer includes three metal patches and one feeding structure; the third layer includes one metal patch and one feeding structure. For these two layers, the metal patches are concatenated to the feeding structures through trapezoid aluminum to form a whole. The height of the two trapezoids is different. Therefore, it can control the gap distance between the two layers. The second layer and third layer are the main components of the proposed antenna. They are two arms of a dipole antenna with the feeding structure. The feeding structure is connected to a 50 Ω coaxial cable. The outer of the coaxial cable is connected to the feeding structure of the second layer, and the inner of the coaxial cable is connected to the feeding structure of the third layer. Normally, the feeding

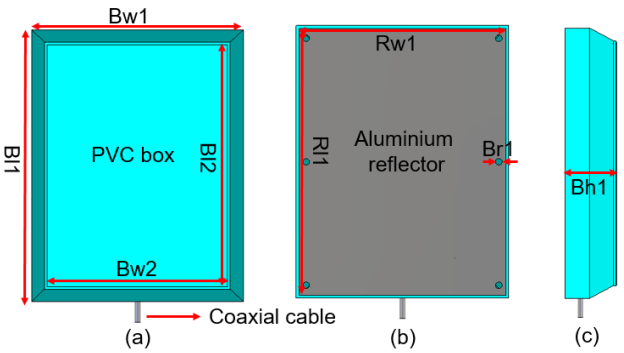


**FIGURE 1.** The outer structure of the proposed antenna. (a) Front view. (b) Back view. (c) Side view.

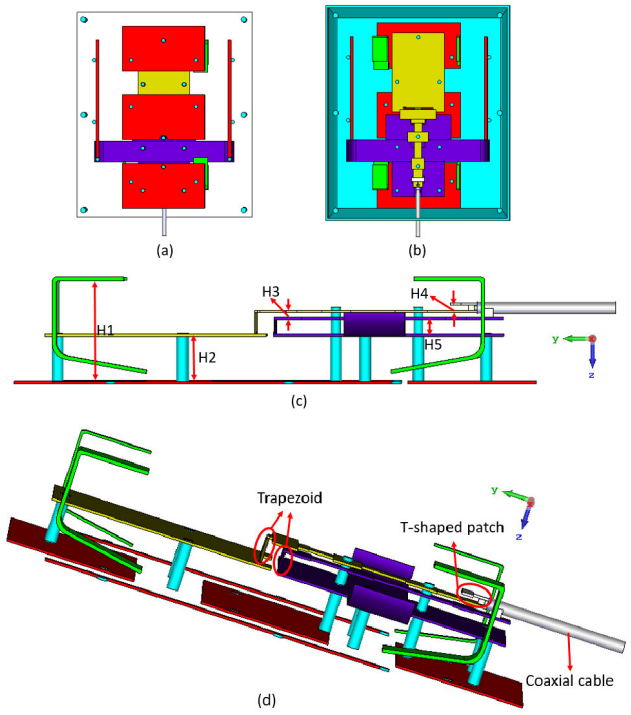


**FIGURE 2.** The inner structure of the proposed antenna. (a) Front view (without box). (b) Back view (without reflector). (c) Side view (without box and reflector). (d) Side view (without box and reflector).

structure is perpendicular to the dipole antenna. However, in this design, the feeding structure is folded and is made parallel to the dipole to minimize the height of the whole antenna. In addition, both ends of the long metal patch in the second layer are bent by 90 degrees to increase the coupling between the first layer and the second layer. The fourth layer is a small T-shaped patch, which is employed to introduce a resonant frequency for the higher frequency band. It is welded to the inner of the coaxial cable through a piece of aluminum. All the four layers are fabricated with 0.8 mm aluminum. The four metal strips are fixed to the reflector by screws and nuts. They are also bent to minimize the height of the antenna. The two thin bent metal strips are made of 0.8 mm aluminum and the two thick bent metal strips are made of 1.2 mm aluminum. In this design, we choose to use aluminum instead of copper due to its low cost, lightweight and highly malleable. The PVC box and cylinders are printed by 3D-Printing technology. Meanwhile, all the aluminum structures are cut by a laser-cutting machine. The detailed dimensions of the proposed antenna are presented in Table 1 which are optimized dimensions as we will discuss later.

## III. EVOLUTION OF THE PROPOSED ANTENNA

The general evolution process includes two stages. The first stage is to cover the three lower bands up to 3.8 GHz. The design process is systematic, and some design parameters can be obtained as follows.

Initially, Antenna 1 was a simple dipole antenna. The two arms of the dipole antenna were made different to achieve

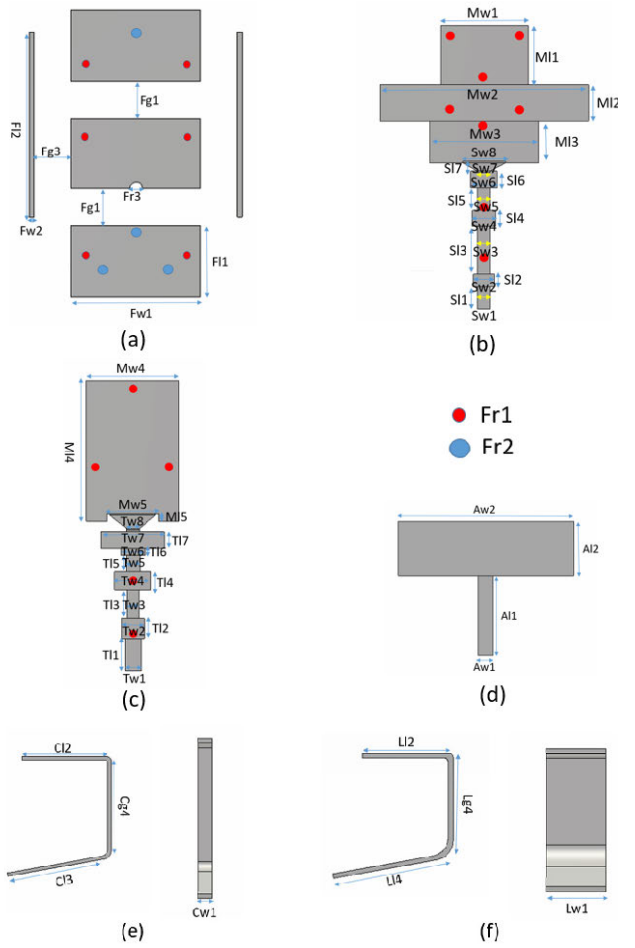


**FIGURE 3.** The detailed structure of the proposed antenna. (a) First layer. (b) Second layer. (c) Third layer. (d) Fourth layer. (e) Side and front view of the thin bent metal strip. (f) Side and front view of the thick bent metal strip.

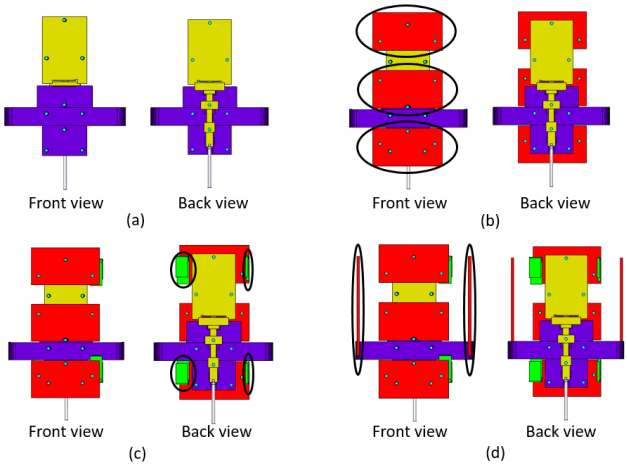


**FIGURE 4.** The evolution of the dual-band antenna. (a) Front and back view of antenna 1. (b) Front and back view of antenna 2. (c) Front and back view of antenna 3. (d) Front and back view of dual-band antenna.

more resonant frequencies. Then, the stepped impedance feeding structure was used to feed the antenna as shown in Fig. 4. As mentioned before, the feeding structure was

**TABLE 1. Dimensions of the proposed antenna.**

| Parameter | Value (mm) | Parame ter | Value (mm) | Parameter | Value (mm) |
|---|---|---|---|---|---|
| Bl1 | 204 | Mw1 | 50 | Tl1 | 17 |
| Bl2 | 185 | Ml1 | 33.5 | Tw1 | 8.6 |
| Bw1 | 175 | Mw2 | 118.4 | Tl2 | 10.8 |
| Bw2 | 160 | Ml2 | 20 | Tw2 | 12.1 |
| Br1 | 5 | Mw3 | 62 | Tl3 | 15.2 |
| Bh1 | 39 | Ml3 | 24 | Tw3 | 6.5 |
| Rw1 | 170.6 | Mw4 | 50 | Tl4 | 9.6 |
| Rl1 | 200 | Ml4 | 75 | Tw4 | 19.9 |
| H1 | 34 | Mw5 | 28 | Tl5 | 8.5 |
| H2 | 15.2 | Ml5 | 4 | Tw5 | 7.4 |
| H3 | 1.6 | Sl1 | 12.7 | Tl6 | 3.8 |
| H4 | 1.7 | Sw1 | 7 | Tw6 | 17.9 |
| H5 | 4.8 | Sl2 | 7 | Tl7 | 8.8 |
| Fl1 | 43.5 | Sw2 | 11.9 | Tw7 | 34.3 |
| Fw1 | 80 | Sl3 | 27.2 | Tw8 | 7 |
| Fl2 | 114 | Sw3 | 7 | Cl2 | 23 |
| Fw2 | 3 | Sl4 | 9 | Cl3 | 26.3 |
| Fg1 | 23 | Sw4 | 13 | Cg4 | 24.33 |
| Fg3 | 22.5 | Sl5 | 12.7 | Cw1 | 2.7 |
| Fr1 | 1.7 | Sw5 | 7 | Ll2 | 23 |
| Fr2 | 2 | Sl6 | 9.4 | Lg4 | 21.8 |
| Aw1 | 1 | Sw6 | 14.9 | Ll4 | 27.9 |
| Al1 | 5.4 | Sl7 | 4.8 | Lw1 | 13.8 |
| Aw2 | 11.9 | Sw7 | 7 | | |
| Al2 | 3.7 | Sw8 | 24.9 | | |

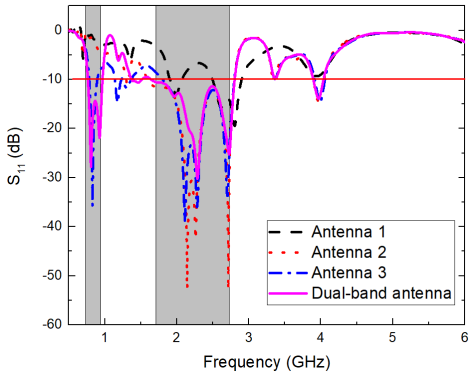


**FIGURE 5. The reflection coefficient of the four reference antennas.**

folded to minimize the height of the antenna. The performance of Antenna 1 is shown in Fig. 5. It is apparent that Antenna 1 has many resonant frequencies, but the bandwidth is narrow. To widen the bandwidth, three aluminum patches were added on the top of the dipole and fixed by the PVC cylinders. They help to widen the bandwidth through coupling between the dipole and three aluminum patches. Therefore, the frequency band 1.7 – 2.7 GHz was achieved. The reflection coefficient of Antenna 2 shows no resonant frequency between 0.8 - 0.96 GHz. As a result, two thick bent metal strips and two thin bent metal strips were introduced to solve this problem, as shown in Fig. 4. However, as shown in Fig. 5, the bandwidth of the first band was not wide enough to cover 0.8 – 0.96 GHz for $S_{11} < -10$ dB. Another two metal strips were introduced to widen the bandwidth. In the end, a dual-band antenna was achieved, which covers

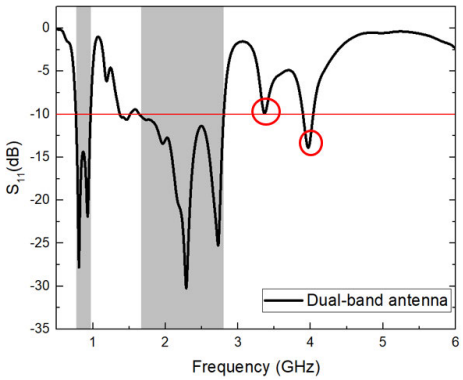


**FIGURE 6. The reflection coefficient of the dual-band antenna.**

0.8 – 0.96 GHz and 1.7 – 2.7 GHz, as shown in Fig. 6. It is easy to find there are two resonant frequencies between 3 and 4 GHz. This means it is possible to realize the band 3.3 – 3.8 GHz through impedance matching. The stepped impedance feeding structure was applied to feed the antenna for the lower frequency band, and it can be used to radiate for the higher frequency band. According to the theory of half-wavelength dipole, the most sensitive parameter for the band 3.3 – 3.8 GHz is Tw4 as shown in Fig. 7. Fig. 8 illuminates that the resistance becomes smaller, and the impedance matching for the band 3.3 – 3.8 GHz becomes better with the increase of Tw4. After few steps of manual tuning, the triple-band performance was achieved as shown in Fig. 9.

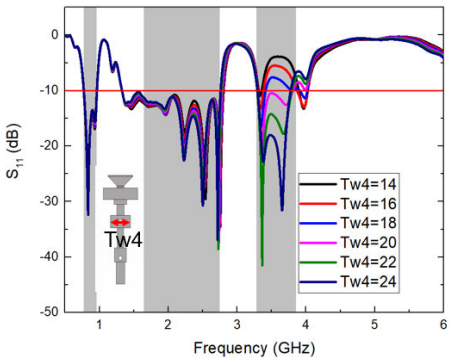


**FIGURE 7. The reflection coefficient of the Tw4 with different length.**

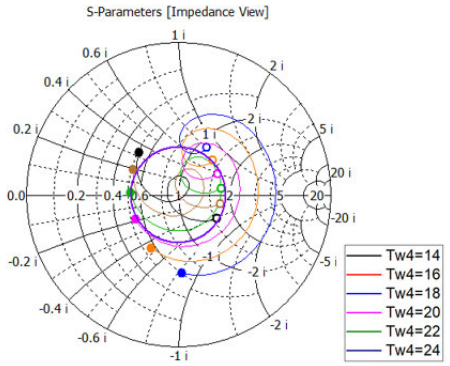


**FIGURE 8. The effect of the Tw4 with different length in Smith chart.**

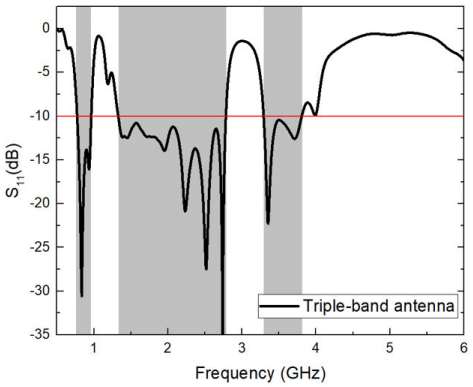


**FIGURE 9.** The reflection coefficient of the triple-band antenna.

The goal of the second stage is to keep the current performance of the three bands at lower frequency ranges and introduce a new resonant frequency for the higher band. Hence, a small T-shaped aluminum patch was put on the top of the feeding structure, and it was soldered with the coaxial cable by a small piece of aluminium. The performance of the antenna is shown in Fig. 10. Then, the task becomes optimizing parameters of the small T-shaped patch and the feeding structure (third layer) to achieve the desired performance of all bands.

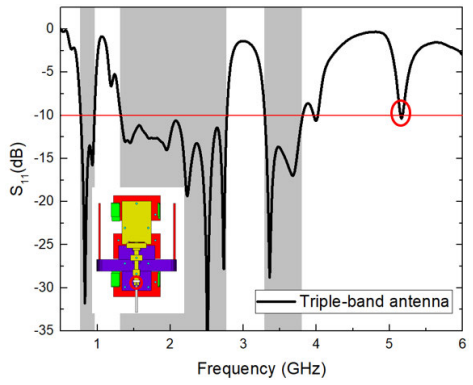


**FIGURE 10.** The reflection coefficient of the triple-band antenna plus small T-shaped patch.

This optimization task is difficult and the widely used local optimizers (e.g., Trust Region Framework in CST Microwave Studio) were firstly employed, but the results were far from satisfactory. Existing global optimizers (e.g., particle swarm optimization) are estimated to cost prohibitive time without a guarantee of success. Therefore, as said in Section I, the state-of-the-art method, PSADEA [1], was used. By using design knowledge to ignore many design parameters for the three bands at lower frequency ranges, the number of critical design parameters were reduced to 19 (Tl1, Tw1, Tl2, Tw2, Tl3, Tw3, Tl4, Tw4, Tl5, Tw5, Tl6, Tw6, Tl7, Tw7, Tw8, Aw1, Al1, Aw2 and Al2). They were optimized to adjust the coupling between the T-shaped patch resonator and the feeding structure of the antenna. The optimization goal is the minimization of the maximum return loss in the newly introduced band (4.8 – 5.0 GHz) subject to having a maximum return loss of less than or equal to −10 dB in the existing bands (i.e. 0.8 – 0.96 GHz, 1.7 – 2.7 GHz and 3.3 – 3.8 GHz). After three days' optimization, PSADEA produced a design with the frequency response shown in Fig. 11, which has met the return loss requirement across all the four bands for sub – 6 GHz 5G operations that is, it covers 0.8 – 0.96, 1.7 – 2.7, 3.3 – 3.8 and 4.8 – 5.0 GHz.

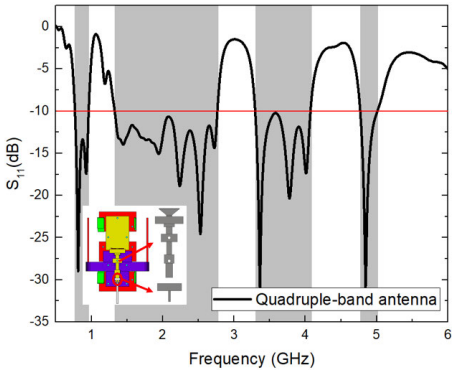


**FIGURE 11.** The reflection coefficient of the quadruple-band antenna.

## IV. THE PROPOSED ANTENNA RESULTS

In order to verify the simulation results, the proposed quadruple-band indoor base station antenna was fabricated and measured, as shown in Fig. 12. The simulation results were obtained using CST microwave studio. Fig. 13 depicts the setup of the measurement; it is accomplished in an anechoic chamber using a Vector Network Analyzer (VNA). Finally, the measurement results of the reflection coefficient, gain and radiation pattern are obtained. The antenna radiation efficiency was obtained using a reverberation chamber.

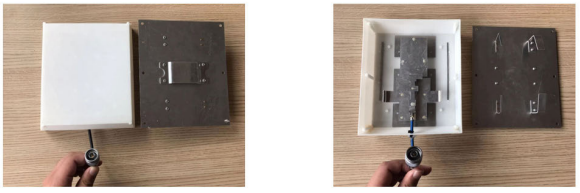


**FIGURE 12.** A prototype of the proposed antenna. (a) Outer view. (b) Inner view.

Fig. 14 illuminates the simulated and measured reflection coefficient. It shows a good agreement between the simulated and measured results. For VSWR $\leq$ 2, the measured impedance fractional bandwidths are 22% (0.77 – 0.96 GHz), 71.8% (1.32 – 2.8 GHz), 21.6% (3.3 – 4.1 GHz) and 4.3% (4.79 – 5.0 GHz) for B1, B2, B3 and B4 respectively.

The simulated and measured realized gains are shown in Fig. 15, where a good agreement between them is observed. The average gain for each band is 5.4 dBi (0.8 – 0.96 GHz), 8.1 dBi (1.7 – 2.7 GHz), 8.5 dBi (3.3 – 3.8 GHz) and 8.1 dBi (4.8 – 5.0 GHz), respectively.

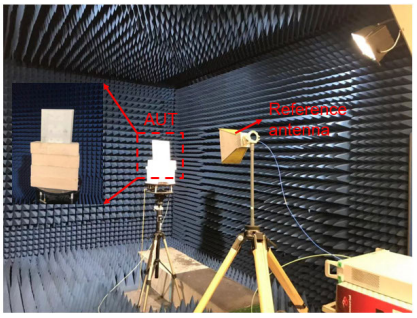


**FIGURE 13.** The setup for the antenna measurement.

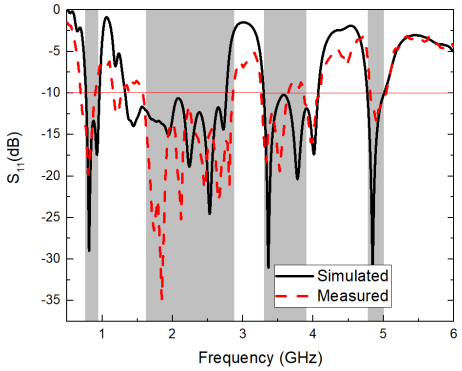


**FIGURE 14.** The simulated and measured reflection coefficient of the proposed quadruple-band antenna.

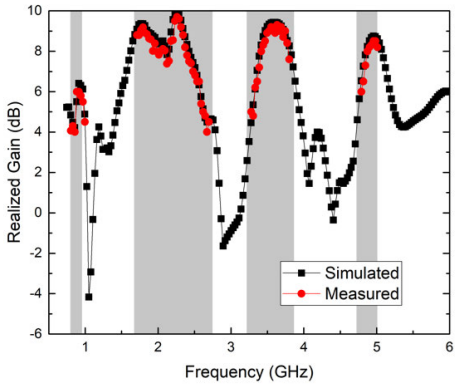


**FIGURE 15.** The simulated and measured maximum gain of the proposed quadruple-band antenna.

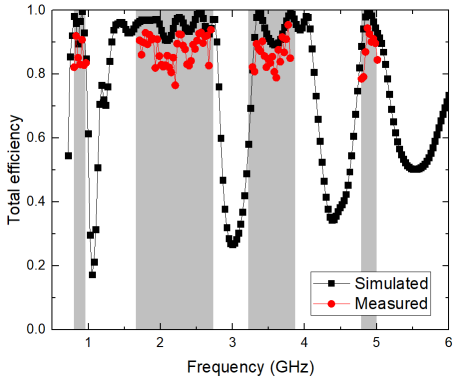


**FIGURE 16.** The simulated and measured total efficiency of the proposed quadruple-band antenna.

Fig. 16 shows the simulated and measured efficiency of the proposed antenna. The overall measured efficiency is over 80%, which is less than the simulated efficiency, which likely due to dielectric loss larger than the one used for simulation.

Fig. 17 depicts the simulated and measured co- and cross-polarized radiation pattern at the start and stop frequencies of each band in H-plane (YOZ plane) and V-plane (XOZ plane). The measured radiation patterns are in good agreement with the simulated ones. For the higher frequency band, the radiation patterns have some distortions. However, for indoor antennas, the radiation pattern requirement is not strictly for the broadside radiation.

Table 2 illuminates the comparison of several multi-band antennas with the proposed antenna. Most of the reference antennas were designed for 2G/3G/4G systems; only one antenna includes the 5G band [17]. It is apparent that the proposed antenna has a relatively small size, especially the height. Meanwhile, it is also the only antenna that covers

**TABLE 2.** Comparison of several multi-band antennas with the proposed antenna.

| Reference | Frequency band (MHz) LB | UB | Bandwidth (%) LB | UB | Gain (dBi) LB | UB | Dimensions ($mm^3$) |
|---|---|---|---|---|---|---|---|
| [15] | 800 – 960 | 1700 – 2700 | 18 (VSWR ≤ 1.5) | 46 (VSWR ≤ 1.5) | 4.6 | 8.7 | 220 × 220 × 42 |
| [16] | 790 – 960 | 1710 – 2170 | 19.4 (VSWR ≤ 1.5) | 23.7 (VSWR ≤ 1.5) | 9.5 | 9 | 255 × 255 × 130 |
| [17] | 700 - 960 | 1700 – 3000 | 31.3 (VSWR ≤ 2) | 55.3 (VSWR ≤ 2) | 5.5 | 8 | 220 × 220 × 100 |
| | 3300 – 3800 | | 14 (VSWR ≤ 2) | | 5.5 | | |
| [24] | 780 – 1100 | 1580 – 2620 | 34 (VSWR ≤ 2) | 49.5 (VSWR ≤ 2) | 7 | 8 | 220 × 220 × 57 |
| [25] | 800 – 980 | 1540 – 2860 | 20 (VSWR ≤ 2) | 60 (VSWR ≤ 2) | 8 | 8 | 360 × 280 × 45 |
| [26] | 790 – 960 | 1710 – 2170 | 19.4 (VSWR ≤ 1.5) | 23.7 (VSWR ≤ 1.5) | 9.3 | 9 | 255 × 255 × 71 |
| **Proposed** | **770 – 960** | **1320 – 2800** | **22 (VSWR ≤ 2)** | **71.8 (VSWR ≤ 2)** | **5.4** | **8.1** | **204 × 175 × 39** |
| | **3300 – 4100** | **4790 – 5000** | **21.6 (VSWR ≤ 2)** | **4.3 (VSWR ≤ 2)** | **8.5** | **8.1** | |

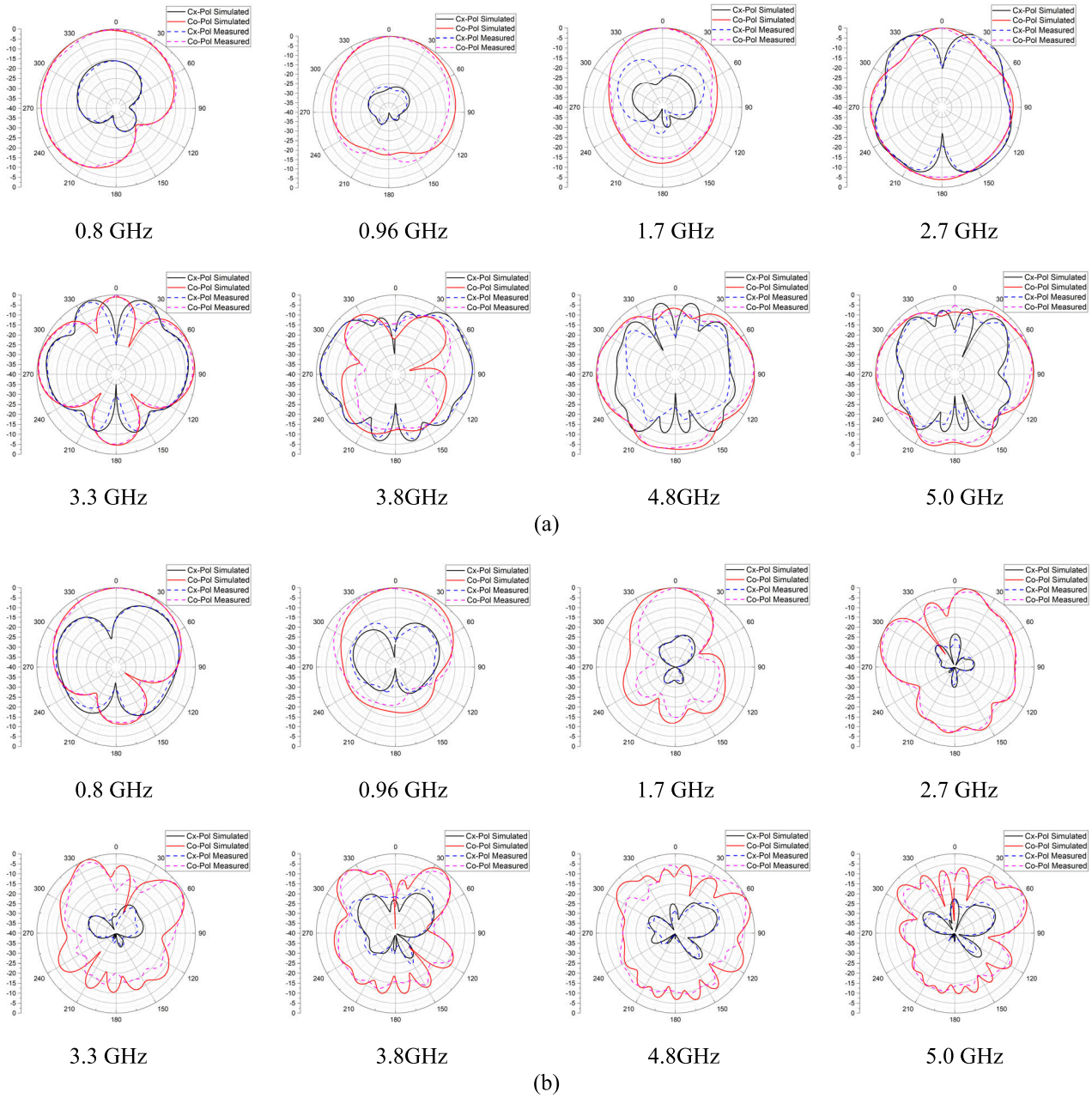


**FIGURE 17.** The simulated and measured co- and cross-polarized radiation pattern. (a) H-plane (YOZ plane). (b) V-plane (XOZ plane).

the four bands used for 2G/3G/4G/5G systems with a good performance.

## V. CONCLUSION

A compact quadruple-band indoor base station antenna for 2G/3G/4G/5G systems has been designed, optimized, fabricated and measured. It covers four wide bands from 0.8 to 0.96 GHz, 1.7 to 2.7 GHz, 3.3 to 3.8 GHz and 4.8 to 5.0 GHz respectively. A plastic case and support frame were fabricated for the antenna to realize a sturdy structure. An asymmetrical dipole antenna and parasitic patches were employed for the lower resonant frequency bands ranging from 0.8 to 0.96 GHz and 1.7 to 2.7 GHz. The stepped impedance feeding structure was used to feed the dipole antenna and meanwhile acted as a radiator for the high frequency band of 3.3 – 3.8 GHz. In addition, a higher resonant frequency has been introduced by a small T-shaped patch to cover 4.8 – 5.0 GHz. The PSADEA method was chosen to optimize 19 critical design parameters to adjust the coupling between the small T-shaped patch and stepped impedance feeding structure. Thus, the proposed quadruple-band performance with VSWR $< 2$ over the frequency band of interest has been obtained. The proposed antenna has achieved low cost and lightweight through aluminum and PVC material manufacturing procedures. It also has a low profile, good performance and sturdy structure simultaneously We believe that the

proposed design will be an excellent candidate for 2G/3G/4G/5G base station antenna systems. For future work, the lower band could be further extended to cover 0.7 – 0.96 GHz to make the antenna suitable for worldwide applications.

## REFERENCES


[1] K. L. Lau and K. M. Luk, "A wide-band monopolar wire-patch antenna for indoor base station applications," *IEEE Antennas Wireless Propag. Lett.*, vol. 4, pp. 155–157, 2005.

[2] Q. Wu, P. Liang, and X. Chen, "A broadband ±45° dual-polarized multiple-input multiple-output antenna for 5G base stations with extra decoupling elements," *J. Commun. Inf. Netw.*, vol. 3, no. 1, pp. 31–37, Mar. 2018.

[3] R. G. Vaughan, "Polarization diversity in mobile communications," *IEEE Trans. Veh. Technol.*, vol. 39, no. 3, pp. 177–186, Aug. 1990.

[4] H. Huang, Y. Liu, and S. Gong, "A broadband dual-polarized base station antenna with sturdy construction," *IEEE Antennas Wireless Propag. Lett.*, vol. 16, pp. 665–668, 2017.

[5] Y. Cui, L. Wu, and R. Li, "Bandwidth enhancement of a broadband dual-polarized antenna for 2G/3G/4G and IMT base stations," *IEEE Trans. Antennas Propag.*, vol. 66, no. 12, pp. 7368–7373, Dec. 2018.

[6] Y. Luo, Q.-X. Chu, and D.-L. Wen, "A plus/minus 45 degree dual-polarized base-station antenna with enhanced cross-polarization discrimination via addition of four parasitic elements placed in a square contour," *IEEE Trans. Antennas Propag.*, vol. 64, no. 4, pp. 1514–1519, Apr. 2016.

[7] Y. Cui, R. Li, and H. Fu, "A broadband dual-polarized planar antenna for 2G/3G/LTE base stations," *IEEE Trans. Antennas Propag.*, vol. 62, no. 9, pp. 4836–4840, Sep. 2014.

[8] W. Chen, H. Lin, H. Ding, Y. Liu, M. Chisala, and Z. Shen, "A low profile broadband dual-polarized base station antenna using folded dipole radiation element," *IEEE Access*, vol. 7, pp. 67679–67685, 2019.

[9] Q. Zhang and Y. Gao, "A compact broadband dual-polarized antenna array for base stations," *IEEE Antennas Wireless Propag. Lett.*, vol. 17, no. 6, pp. 1073–1076, Jun. 2018.

[10] L.-H. Wen, S. Gao, Q. Luo, C.-X. Mao, W. Hu, Y. Yin, Y. Zhou, and Q. Wang, "Compact dual-polarized shared-dipole antennas for base station applications," *IEEE Trans. Antennas Propag.*, vol. 66, no. 12, pp. 6826–6834, Dec. 2018.

[11] A. Alieldin, Y. Huang, S. J. Boyes, M. Stanley, S. D. Joseph, and B. Al-Juboori, "A dual-broadband dual-polarized fylfot-shaped antenna for mobile base stations using MIMO over-lapped antenna subarrays," *IEEE Access*, vol. 6, pp. 50260–50271, 2018.

[12] Y. He, Z. Pan, X. Cheng, J. Qiao, and M. M. Tentzeris, "A novel dual-band, dual-polarized, miniaturized and low-profile base station antenna," *IEEE Trans. Antennas Propag.*, vol. 63, no. 12, pp. 5399–5408, Dec. 2015.

[13] L. Y. Nie, X. Q. Lin, Y. J. Chen, J. Zhang, B. Wang, Z. Q. Yang, and Y. Fan, "A low-profile coplanar dual-polarized and dual-band base station antenna array," *IEEE Trans. Antennas Propag.*, vol. 66, no. 12, pp. 6921–6929, Dec. 2018.

[14] H. Huang, Y. Liu, and S. Gong, "A novel dual-broadband and dual-polarized antenna for 2G/3G/LTE base stations," *IEEE Trans. Antennas Propag.*, vol. 64, no. 9, pp. 4113–4118, Sep. 2016.

[15] Y. Zhao, C. Rakluea, T. Hongnara, and S. Chaimool, "A compact dual-broadband multiple-input multiple-output (MIMO) indoor base station antenna for 2G/3G/LTE systems," *IEEE Access*, vol. 7, pp. 82238–82245, 2019.

[16] Y. He, W. Tian, and L. Zhang, "A novel dual-broadband dual-polarized electrical downtilt base station antenna for 2G/3G applications," *IEEE Access*, vol. 5, pp. 15241–15249, 2017.

[17] A. Alieldin, Y. Huang, S. J. Boyes, M. Stanley, S. D. Joseph, Q. Hua, and D. Lei, "A triple-band dual-polarized indoor base station antenna for 2G, 3G, 4G and Sub-6 GHz 5G applications," *IEEE Access*, vol. 6, pp. 49209–49216, 2018.

[18] B. Liu, M. O. Akinsolu, N. Ali, and R. Abd-Alhameed, "Efficient global optimisation of microwave antennas based on a parallel surrogate model-assisted evolutionary algorithm," *IET Microw., Antennas Propag.*, vol. 13, no. 2, pp. 149–155, Feb. 2019.

[19] M. O. Akinsolu, B. Liu, V. Grout, P. I. Lazaridis, M. E. Mognaschi, and P. Di Barba, "A parallel surrogate model assisted evolutionary algorithm for electromagnetic design optimization," *IEEE Trans. Emerg. Topics Comput. Intell.*, vol. 3, no. 2, pp. 93–105, Apr. 2019.

[20] B. Liu, H. Aliakbarian, Z. Ma, G. A. E. Vandenbosch, G. Gielen, and P. Excell, "An efficient method for antenna design optimization based on evolutionary computation and machine learning techniques," *IEEE Trans. Antennas Propag.*, vol. 62, no. 1, pp. 7–18, Jan. 2014.

[21] B. Liu, S. Koziel, and N. Ali, "SADEA-II: A generalized method for efficient global optimization of antenna design," *J. Comput. Des. Eng.*, vol. 4, no. 2, pp. 86–97, 2017.

[22] V. Grout, M. O. Akinsolu, B. Liu, P. I. Lazaridis, K. K. Mistry, and Z. D. Zaharis, "Software solutions for antenna design exploration: A comparison of packages, tools, techniques, and algorithms for various design challenges," *IEEE Antennas Propag. Mag.*, vol. 61, no. 3, pp. 48–59, Jun. 2019.

[23] B. Liu, Q. Zhang, and G. G. E. Gielen, "A Gaussian process surrogate model assisted evolutionary algorithm for medium scale expensive optimization problems," *IEEE Trans. Evol. Comput.*, vol. 18, no. 2, pp. 180–192, Apr. 2014.

[24] W. X. An, H. Wong, K. L. Lau, S. F. Li, and Q. Xue, "Design of broadband dual-band dipole for base station antenna," *IEEE Trans. Antennas Propag.*, vol. 60, no. 3, pp. 1592–1595, Mar. 2011.

[25] Y. Cui, R. Li, and P. Wang, "Novel dual-broadband planar antenna and its array for 2G/3G/LTE base stations," *IEEE Trans. Antennas Propag.*, vol. 61, no. 3, pp. 1132–1139, Mar. 2013.

[26] G. Cui, S.-G. Zhou, G. Zhao, and S.-X. Gong, "A compact dual-band dual-polarized antenna for base station application," *Prog. Electromagn. Res. C*, vol. 64, pp. 61–70, May 2016.


**QIANG HUA** received the B.Sc. degree in communication engineering from University of Liverpool, Liverpool, U.K., in 2016, and the M.Sc. degree in digital signal processing from The University of Manchester, Manchester, U.K., in 2017. He is currently pursuing the Ph.D. degree in base station antennas with University of Liverpool. His current research interest includes the base station antenna design for 5G in wireless communications.

**YI HUANG** (S'91–M'96–SM'06) received the B.Sc. degree in physics from Wuhan University, China, in 1984, the M.Sc. (Eng.) degree in microwave engineering from NRIET, Nanjing, China, in 1987, and the D.Phil. degree in communications from the University of Oxford, U.K., in 1994. He has been conducting research in the areas of wireless communications, applied electromagnetics, radar and antennas, since 1987. His experience includes 3 years spent with NRIET as a Radar Engineer and various periods with the Universities of Birmingham, Oxford, and Essex, U.K., as a Member of Research Staff. He was a Research Fellow with British Telecom Labs, in 1994, and then joined the Department of Electrical Engineering & Electronics, University of Liverpool, U.K., as a Faculty, in 1995, where he is currently a Full Professor in wireless engineering, the Head of the High Frequency Engineering Group, and the Deputy Head of the Department. He has published more than 350 refereed articles in leading international journals and conference proceedings, and authored *Antennas: From Theory to Practice* (John Wiley, 2008) and *Reverberation Chambers: Theory and Applications to EMC and Antenna Measurements* (John Wiley, 2016). He has received many research grants from research councils, government agencies, charity, EU and industry, acted as a consultant to various companies, and served on a number of national and international technical committees and been an Editor, Associate Editor or Guest Editor of five international journals. He has been a keynote/invited speaker and organizer of many conferences and workshops (e.g. WiCom 2006, 2010, IEEE iWAT2010, LAPC2012, and EuCAP2018). He is currently the Editor-in-Chief of *Wireless Engineering and Technology*, an Associate Editor of the IEEE Antennas and Wireless Propagation Letters, U.K., and Ireland Rep to European Association of Antenna and Propagation (EurAAP), a Fellow of IET and a Senior Fellow of HEA.

**CHAOYUN SONG** (M'16) received the M.Sc. and Ph.D. degrees in electrical engineering and electronics from University of Liverpool (UoL), Liverpool, U.K., in 2013 and 2017, respectively. He was a Research Assistant and an Antenna Design Engineer with UoL and the BAE systems, Chelmsford, U.K., from 2015 to 2016. He is currently a Postdoctoral Research Associate UoL. He has authored or coauthored more than 45 articles (including 20 IEEE Transactions) in internationally refereed journals and conference proceedings. He has filed five US, EU, and U.K. patents. His current research interests include liquid antennas, novel materials, wireless energy harvesting, rectifying antennas, wireless power transfer, global navigation satellite system antennas and anti-jamming technologies, and smart sensors for the Internet of Things. He was a recipient of many international awards such as the winner of the IET Present Around the World Competition, in 2016, and the EW Bright-Sparks Award for outstanding electronic engineers under age 30 in U.K., in 2018. He was also a recipient of the BAE Systems Chairman's Award, in 2017 for the innovation of next generation global navigation satellite system antennas. He has been a regular Reviewer of more than ten international journals, including *Applied Physics Letters*, *Scientific Reports*, the IEEE TRANSACTIONS ON ANTENNAS AND PROPAGATION, the IEEE TRANSACTIONS ON INDUSTRIAL ELECTRONICS, the IEEE TRANSACTIONS ON MICROWAVE THEORY AND TECHNIQUES, the IEEE TRANSACTIONS ON CIRCUITS AND SYSTEMS I: REGULAR PAPERS, the IEEE ANTENNAS AND WIRELESS PROPAGATION LETTERS, and the IEEE SENSORS LETTERS.

**MOBAYODE O. AKINSOLU** (M'16) received the M.Sc. degree (Hons.) in electrical and electronic engineering from the University of Bradford, U.K., in 2014, after his undergraduate studies and compulsory national service in Nigeria. He is currently pursuing the Ph.D. degree, awardee in recognition of a joint project, from Wrexham Glyndŵr University, U.K., and the University of Birmingham, U.K. His Ph.D. research focuses on electromagnetic design automation using surrogate model-assisted evolutionary algorithms. He was a Research Fellow (industrial attaché) and a Visiting Researcher with the National Space Research and Development Agency, Nigeria, and the RFID Research Centre, African University of Science and Technology, Nigeria, respectively, until 2016. He is currently a Lecturer in electronic and communication engineering with Wrexham Glyndŵr University, U.K. He is a member of the IET and a Registered Electrical Engineer with COREN.

**BO LIU** (M'15–SM'17) received the B.S. degree from Tsinghua University, China, in 2008, and the Ph.D. degree with the MICAS Laboratories, University of Leuven (KU Leuven), Belgium, in 2012. From 2012 to 2013, he was a Humboldt Research Fellow. He was with the Technical University of Dortmund, Germany. In 2013, he was a Lecturer with Wrexham Glyndwr University, U.K., where he was a Reader (tenured Associate Professor) in computer-aided design, in 2016. He has authored or coauthored one book and more than 60 articles in international journals, edited books, and conference proceedings. His research interests include AI-driven design methodologies of analog/RF integrated circuits, microwave devices, MEMS, evolutionary computation, and machine learning.

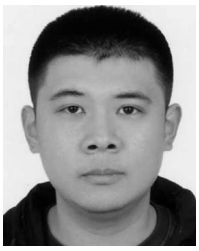

**TIANYUAN JIA** received the B.Eng. degree in telecommunications engineering from Xi'an Jiaotong-Liverpool University (XJTLU), Suzhou, China, in 2012, and the M.Sc. degree in communications and signal processing from Imperial College London, London, U.K., in 2013. He is currently pursuing the Ph.D. degree in electrical engineering and electronics with the University of Liverpool, Liverpool, U.K.

His current research interests include reverberation chamber measurement techniques, 5G over-the-air testing, propagation channel modelling and emulation, electromagnetic compatibility testing, statistical electromagnetics, and localization techniques.

**QIAN XU** received the B.Eng. and M.Eng. degrees from the Department of Electronics and Information, Northwestern Polytechnical University, Xi'an, China, in 2007 and 2010, respectively, and the Ph.D. degree in electrical engineering from the University of Liverpool, U.K., in 2016.

He was as a RF Engineer in Nanjing, China, in 2011, an Application Engineer with CST Company, Shanghai, China, in 2012. His work at University of Liverpool was sponsored by Rainford EMC Systems Ltd. (now part of Microwave Vision Group) and the Centre for Global Eco-Innovation. He is currently an Associate Professor with the College of Electronic and Information Engineering, Nanjing University of Aeronautics and Astronautics, China. He has authored the book *Anechoic and Reverberation Chambers: Theory, Design, and Measurements* (Wiley-IEEE, 2019). His research interests include statistical electromagnetics, reverberation chamber, computational electromagnetics, and anechoic chamber.

**AHMED ALIELDIN** (M'16) received the B.Sc. degree in radar engineering from the Military Technical College, Egypt, in 2005, the M.Sc. (Eng.) degree in antenna and microwave Propagation from the University of Alexandria, Egypt, in 2013, and the Ph.D. degree in antennas and electromagnetics from the University of Liverpool, U.K., in 2019. His academic research activities and Ph.D. were centred on antenna designing and measurements with an emphasis on mobile communication applications.

In addition to work in academia, he also held various positions throughout more than ten years working in the industry. He is currently a Senior RF Research Scientist with Benha Electronics Company, where he is involved in projects of national importance. He authored or coauthored many articles in leading international journals and conference proceedings. He has also filed a patent. His current research interests include novel textile antennas, multiple-input multiple-output antennas, base station antennas, satellite antennas, transparent antennas, and phased-MIMO radar antennas.

Dr. Alieldin served as a session chair in many international conferences and serves as a Technical Reviewer for leading academic journals and conferences.